Eur. Phys. J. E **23**, 295–303 (2007)
DOI 10.1140/epje/i2007-10191-6

THE EUROPEAN PHYSICAL JOURNAL E

Miscibility in poly(L-lactide)-b-poly(ε-caprolactone) double crystalline diblock copolymers

E. Laredo[1,a], N. Prutsky[1], A. Bello[1], M. Grimau[2], R.V. Castillo[2], A.J. Müller[2], and Ph. Dubois[3]

[1] Physics Department, Universidad Simón Bolívar, Apartado 89000, Caracas 1080 A, Venezuela
[2] Materials Science Department, Universidad Simón Bolívar, Apartado 89000, Caracas 1080 A, Venezuela
[3] Laboratory of Polymeric and Composite Materials (LPCM), University of Mons-Hainaut, Place du Parc 20, 7000 Mons, Belgium

Received 29 March 2007
Published online: 8 August 2007 – © EDP Sciences / Società Italiana di Fisica / Springer-Verlag 2007

Abstract. Thermally stimulated depolarization currents, TSDC, wide-angle X-ray scattering, WAXS, differential scanning calorimetry, DSC, and polarized light optical microscopy, PLOM, have been used to examine poly(L-lactide)-*b*-poly(ε-caprolactone) diblock copolymers in a wide composition range. Both components are crystallizable and the miscibility in the amorphous phase has been determined from the behavior of the primary relaxations which are the dielectric manifestation of the glass transition, and also from the superstructural morphology revealed by PLOM and the compositional dependence of the melting points as determined by DSC. Distinct segmental mobilities in the amorphous phase which can be well resolved by TSDC are present; the α mode of the slower component shifts to lower temperatures as the PCL content increases while the glass transition of neat PCL is present for all compositions. A relaxation times bimodal distribution is apparent for PCL-rich copolymers. The composition dependence of the multiple glass transitions detected in these weakly segregated copolymers are predicted by the self-concentration model for a miscible blend made of components with a large T_g contrast.

PACS. 64.70.Pf Glass transitions – 77.22.Gm Dielectric loss and relaxation – 77.84.Jd Polymers; organic compounds – 64.70.Nd Structural transitions in nanoscale materials

1 Introduction

In diblock copolymers, phase segregation and the subsequent formation of nanoscale morphologies are caused by repulsion between the bonded chains. When the diblock copolymer is made from two crystallizable blocks interesting situations are found. The mobility and self-assembly of the two amorphous phases might be constrained by the presence of crystallites whose abundance depends on the copolymer composition. Additionally, if one or both components of the block copolymer are polar, the molecular dynamics at different scales can be followed by dielectric techniques as a function of temperature, composition, crystallinity and morphology. Even though several studies on the properties of double crystalline diblock copolymers have been published [1–10], their detailed behavior is still not thoroughly understood. A couple of recent reviews have dealt with the morphology, nucleation and crystallization of these materials [11,12].

The poly(L-lactide)-*b*-poly(ε-caprolactone), PLLA-*b*-PCL, diblock copolymers can exhibit interesting properties for biological applications which take advantage of the susceptibility to degradation of the PLLA block and the relative stability of the PCL one. These copolymers are in the weak segregation regime and their melt structure depends on composition; however, the microdomain structure is dominated by crystallization [6,9,10]. Previous studies on this system [9,10] by various techniques such as time-resolved X-ray techniques, polarized light optical microscopy, PLOM, and differential scanning calorimetry, DSC, showed that for most compositions of the copolymers they were miscible in the melt. Such miscibility resembles that of a polymer blend and therefore the Lodge and McLeish self-concentrations model [13] might be applied to describe the dynamics of this system. Previously, this model has been successfully used to interpret the segmental dynamics in disordered styrene-isoprene tetrablock copolymers [14,15]. The crystallization kinetics pointed to instantaneous nucleation of the PLLA with 3D superstructures and as the temperature decreased to 30 °C the PCL block was able to crystallize within the PLLA negative spherulites (*i.e.*, within the intra-spherulitic regions). The PCL crystallization rate was much slower than in neat PCL.

[a] e-mail: elaredo@usb.ve; http://www.fimac.labd.usb.ve

Table 1. Molecular characteristics of the block copolymers and homopolymers.

Sample code	PLLA/PCL exp. comp.[a]	$M_{n,exp}$ PLLA block	$M_{n,exp}$[c] PCL block	I[d]
86PLLA	100/0	86000[c]	–	1.8
24PLLA	100/0	23900[b]	–	1.1
$L_{93}C_{07}$	93/07	15700[b]	1700	1.3
$L_{81}C_{19}$	81/19	16700[b]	3900	1.3
$L_{55}C_{45}$	55/45	9500[b]	8100	1.4
$L_{32}C_{68}$	32/68	6900[b]	14900	1.4
$L_{10}C_{90}$	10/90	2400[b]	21500	1.4
29PCL	0/100	–	28900	1.3

([a]) Experimental composition as determined by ^{1}H NMR.
([b]) Calculated M_n estimated by ^{1}H NMR for the PLLA block knowing the M_n of the PCL block determined by SEC in g/mol.
([c]) Experimental M_n estimated by SEC in g/mol.
([d]) Polydispersity index of the final copolymer (determined by SEC).

The previous studies on the PLLA-*b*-PCL diblock copolymers have been devoted to the characterization of the crystalline phases and little information from classical techniques has been gathered on the miscibility or the dynamics of the amorphous phase. In this work, the miscibility of the amorphous phases in the whole composition range is studied by its effect on the dielectric relaxations of the two polar components by using thermally stimulated depolarization currents, TSDC, technique. Additionally, wide-angle X-ray scattering, WAXS, is used to evaluate the crystallinity of both phases. DSC and PLOM were also employed to complement the TSDC results.

2 Experimental section

2.1 Materials

The synthesis of the PLLA-*b*-PCL diblock copolymers was performed by controlled/"living" sequential block copolymerization in toluene solution [16]. The diblock copolymer nomenclature used here denotes the PLLA block as L and the PCL block as C, subscripts indicate the approximate bulk composition in weight %. The compositions studied were $L_{93}C_{07}$, $L_{81}C_{19}$, $L_{55}C_{45}$, $L_{32}C_{68}$ and $L_{10}C_{90}$ and their molecular weight characterization data obtained by ^{1}H NMR and size exclusion chromatography (SEC) are summarized in Table 1. Molecular weights and molecular-weight distribution were calculated with reference to polystyrene standards. The absolute average-number molecular weight, $M_{n,exp}$, of PCL was calculated using a universal calibration curve and polystyrene standards in THF at 35 °C. The samples for TSDC studies were prepared by compression moulding at 190 °C. Two neat PLLA samples were employed for DSC studies: 24PLLA and 86PLLA (for homopolymers the prefix indicate the approximate number average molecular weight in kg/mol). The low-molecular-weight sample (*i.e.*, 24PLLA) was synthesized employing similar conditions as the block copolymers. Unfortunately, suitable samples for TSDC studies require films of uniform thickness, disk shaped and without moulding defects. Such good-quality films were impossible to prepare with the 24PLLA because it crystallizes during quenching and the films became too brittle. In view of this, TSDC experiments were performed on a commercial PLLA sample supplied by Purac Biochem whose molecular characteristics are also reported in Table 1. This neat PLLA sample (*i.e.*, 86PLLA) used in the TSDC experiments was completely amorphous as determined from its WAXS spectrum. The $L_{10}C_{90}$ composition was studied only by WAXS as the films were too irregular for the TSDC experiments.

2.2 TSDC experiments

Compression-moulded samples of about 120 μm thickness and 20 mm in diameter were polarized in a cryostat with a controlled dry He atmosphere. The polarizing fields were about 8 MV/m and the polarization temperature was chosen to allow the species under study to orient during the polarization step. The dipolar oriented state is frozen by quenching to liquid-nitrogen temperature where the field can be switched off. The sample is then heated at a linear rate equal to 0.070 K/s, while the depolarization current is recorded with a Keathley 642 electrometer. The sensitivity of our detection system is 10^{-16} A with an excellent signal-to-noise ratio [17].

2.3 WAXS experiments

An automatic Panalytical diffractometer with Ni-filtered Cu $K\alpha$ radiation was used to calculate the degree of crystallinity of the compression-moulded samples from the WAXS patterns. Crystallinity of both components is determined by the decomposition of the experimental curve into the Bragg crystalline peaks described below in addition to the amorphous halos of both components of the double-crystalline copolymer. The spectra were recorded at room temperature from samples with the same thermal history as the films that were used for the TSDC studies.

2.4 DSC experiments

A Perkin-Elmer DSC-7 differential scanning calorimeter was employed. Compression-moulded films were encapsulated in aluminium pans (mass was approximately 5 mg in all cases). The calibration was performed with indium and hexatriacontane and all tests were run employing ultra pure nitrogen as purge gas. Samples were cooled from 25 °C down to −20 °C and then first DSC heating scans from −20 °C to 190 °C were performed at 10 °C/min.

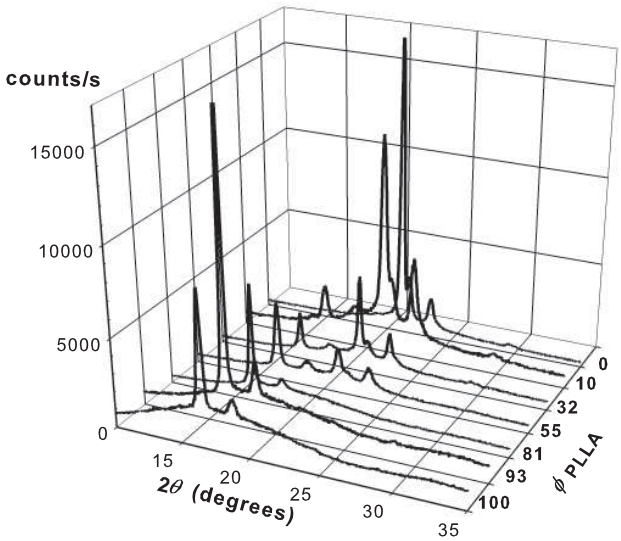

Fig. 1. WAXS patterns (Cu λ $K\alpha$) at room temperature for PLLA-*b*-PCL copolymers with compositions from 100%PLLA (front) to 100% PCL (back).

2.5 Polarized light optical microscopy experiments

Thin films were prepared between microscope cover slips by melting the polymer at 190 °C for 3 min and then they were quickly cooled to the isothermal crystallization temperature in a Linkam TP-91 hot-stage. The samples were observed between crossed polarizers in a Zeiss MC-80 optical microscope equipped with a camera system. Additionally, thin sections of compression-moulded films were observed at room temperature. In order to enhance contrast and determine the sign of the spherulites, a λ wave plate was inserted between the polarizers.

3 Results and discussion

3.1 WAXS results

The WAXS results presented in Figure 1 for the whole bulk composition range from pure 24PLLA to pure 29PCL show the semicrystalline character of both homopolymers. For PCL the degree of crystallinity decreases by the addition of increasing amounts of the other block.

PCL crystallizes in the orthorhombic $P2_12_12_1$ space group with $a = 7.496$ Å, $b = 4.974$ Å and $c = 17.297$ Å [18]. The most intense PCL Bragg reflections, when using Cu $K\alpha$ radiation, are located at 2θ values of 15.64° (102), 21.40° (110), 22.05° (111), 23.70° (200), 24.3° (201) and 29.85° (210). The α form of PLLA crystallizes in the same space group but the cell parameters are $a = 10.66$ Å, $b = 6.16$ Å and $c = 28.88$ Å [19]. The main PLLA reflections are the (110) and (200) at $2\theta = 16.63°$ ($d = 5.326$ Å) and a wider peak at 18.92° which comprises the (014), (113) and (203) reflections ($d = 4.687, 4.666, 4.663$ Å).

The decomposition of the WAXS trace in the amorphous and crystalline contributions of both components allows the calculation of the crystallinity degree, X_c, at room temperature for as-given films. The variation of X_c as a function of the amount of the PLLA nominal composition, ϕ_{PLLAnom}, is presented in Figure 2. There, it is shown that the PLLA is semicrystalline for the whole composition range, while PCL becomes amorphous for $\phi_{\mathrm{PLLAnom}} \geq 80\%$.

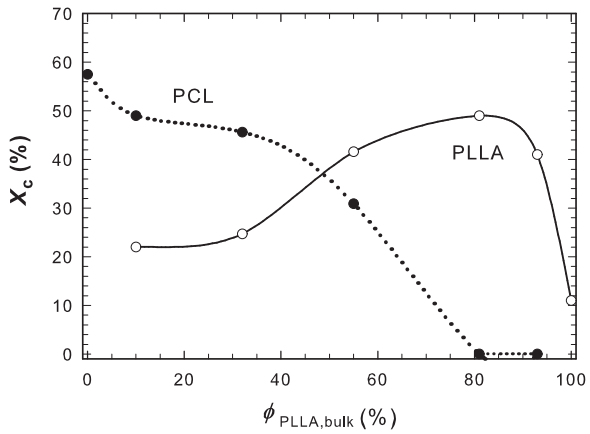

Fig. 2. Variation of crystallinity degrees with bulk composition of the two components of the diblock copolymer PLLA-*b*-PCL.

By polarized optical microscopy, PLOM, it has been shown that these copolymers present superstructures of mixed spherulites, *i.e.*, that the PCL crystallization which occurs at lower temperatures than the PLLA preserves the morphology established by the PLLA previously formed spherulites. PLLA and PCL lamellae are separated by PLLA/PCL mixed amorphous regions. Evidences of this behavior will be presented below.

3.2 TSDC results

The low-temperature TSDC spectra are shown in Figure 3. The films have been polarized at 150 K in order to avoid any interference from the more intense peaks that occur at higher temperature. These wide multicomponent peaks are caused by the local mobilities of the carbonyl group in both polymers. These peaks have been decomposed in Debye modes characterized by single Arrhenius relaxation times, $\tau = \tau_0 \exp(E_A/kT)$ by using a simulated annealing direct signal analysis based on a Monte Carlo algorithm [20]. An example of this decomposition is shown in Figure 4 for the $L_{55}C_{45}$ block copolymer. Figure 4(a) shows the experimental points and the fitted curve, together with the position and amplitude of the Debye processes the sum of which reproduces best the experimental curve. The histogram of the contributions to the total polarization of each elementary mode drawn in Figure 4(b) can be fitted with 3 Gaussian distributions (γ_1, γ_2 and β) evidencing the multicomponent character of this broad peak. For neat 29PCL these three local modes are comparable, while for neat 86PLLA the β mode is significantly the most intense, as seen in Figure 3. The Arrhenius activation energies of each relaxation do

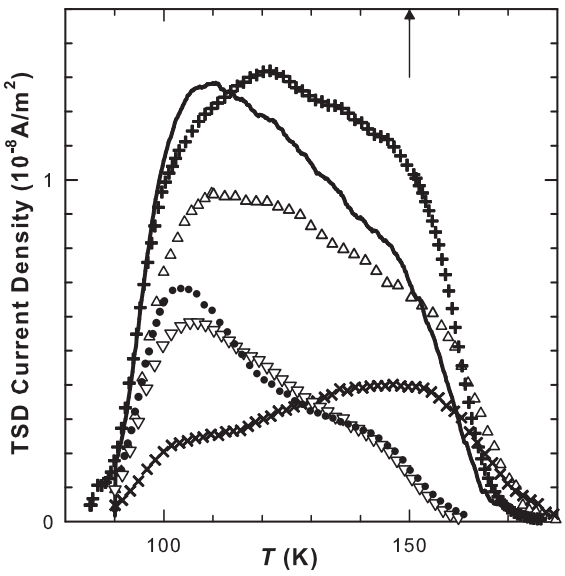

Fig. 3. Low-temperature TSDC spectra for the diblock copolymers PLLA-*b*-PCL for various bulk compositions; $T_p = 150\,\mathrm{K}$. +: 0/100; △: 32/68; ———: 55/45; ▽: 81/19; •: 93/07; ×: 100/0.

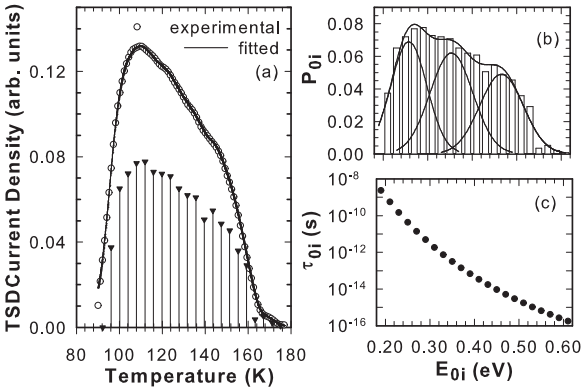

Fig. 4. Simulated annealing direct signal analysis of the low-temperature modes of the 55/45 PLLA-*b*-PCL block copolymer: (a) TSDC trace and positions of the Debye modes. (b) Energy histogram of the contributions to the total polarization. (c) Variation of the pre-exponential Arrhenius factor as a function of the activation energy of each Debye mode.

not change significantly with composition the mean values being $E_{\gamma_1} = (0.25 \pm 0.01)\,\mathrm{eV}$, $E_{\gamma_2} = (0.35 \pm 0.01)\,\mathrm{eV}$, $E_\beta = (0.49 \pm 0.01)\,\mathrm{eV}$.

When caused by small amplitude local motions in the amorphous phase, the secondary relaxations have often been found to be insensitive to the presence of a second polar component; this is obviously not the case in these block copolymers. In Figure 3 very significant changes are observed in the profile and intensity of the low temperature modes on sweeping the composition range, even though the mean activation energy is not affected. Starting from the neat 86PLLA (which has a higher molecular weight than the PLLA in the copolymers) it is found that the β transition has a higher intensity than the γ modes. The copolymer that contains only 7% PCL exhibits a TSDC profile where the intensity ratio of the β and γ modes is inverted as compared to 86PLLA. As the PCL concentration increases the TSDC profile, which is the sum of the local modes of both PLLA and PCL, flattens, thus approaching the profile of the neat PCL low-temperature spectrum.

Simultaneously, the crystallinity of the PLLA component proved to increase significantly with PCL content in the copolymer. The decrease in the strength of the β mode which is caused by the motions of longer range than those at the origin of the γ modes, seems related to the crystallinity increase as the small amount of PCL (where the strength of the γ and β modes are comparable) cannot justify the change in the profile of the peaks. The presence of the PLLA crystalline lamellae imposes constraints to the nearest mode of the α relaxation associated to the glass transition of the polymer. In the classification proposed by Ngai and Paluch [21] for secondary relaxations in amorphous polymers many effects are reviewed in order to distinguish a true Johari-Goldstein β mode [22] from a local intramolecular motion. Constraints imposed on the molecular motions by the existence of crystal lamellae have not been considered. The profile variations observed here which are mainly due to the decrease in the intensity, *i.e.*, the number of orientable dipoles, of the PLLA β relaxation points to an origin linked to a motion involving all parts of the basic structural unit. For PCL, detailed broad-band dielectric spectroscopy experiments [23] have shown the existence at high temperatures of a merging of the α and β relaxations which has been considered as a necessary condition for genuine JG relaxation [21]. Another feature that indicates that the relaxation time characteristic of each elementary mode that composes the high-temperature tail of the β mode are not having an Arrhenius behavior is the low values obtained for the inverse frequency factor, τ_0 as seen in Figure 4(c). This is indicative of a switching from an Arrhenius to a Vogel-Tammann-Fulcher, VTF, temperature dependence for the relaxation times, $\tau_{\mathrm{VTF}} = \tau_0' \exp\left(E_{\mathrm{VTF}}/k(T - T_{\mathrm{VTF}})\right)$.

Above 170 K the TSDC spectrum for each copolymer composition shows a complex suite of more intense peaks which are characteristic of glass transitions. In Figure 5 the high-temperature spectra for all the compositions studied here are represented and an abundance of high-temperature modes is observed. The two homopolymers have very distant glass transition temperatures whose dielectric manifestations are the α peaks for 29PCL and 86PLLA at 207 K and 330 K, respectively. This T_g contrast, $\Delta T_g = 123\,\mathrm{K}$, allows a thorough study of the miscibility of the amorphous phase in the nearly disordered block copolymers and its behavior with composition. The first important result is that for all compositions the α_{PCL} relaxation for neat PCL is present in the TSDC spectrum of the diblock copolymers. The presence of a relaxation mode that does not shift with composition over such wide composition variations, might be at first interpreted as the indication of a phase segregation in the amorphous regions, where the PCL chains are undergoing

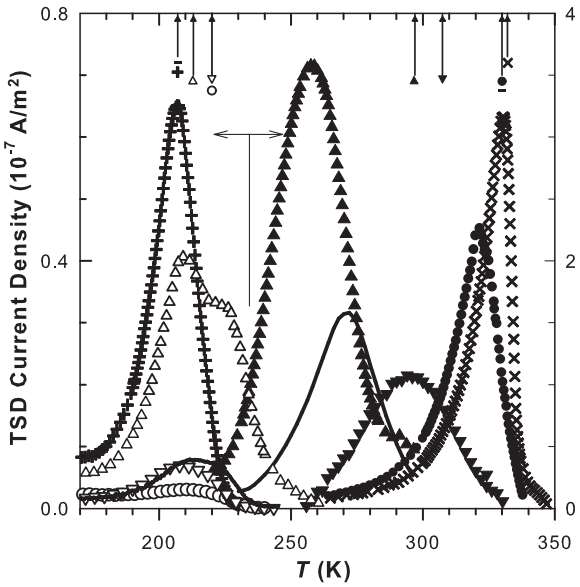

Fig. 5. High-temperature TSDC spectra for the diblock copolymers PLLA-*b*-PCL for various bulk compositions and polarization temperatures; +: 0/100; △, ▲: 32/68; ——: 55/45; ▽, ▼: 81/19; ○, ●: 93/07; ×: 100/0. Left scale for open symbols, right scale for filled symbols. The polarization temperatures are shown by vertical arrows.

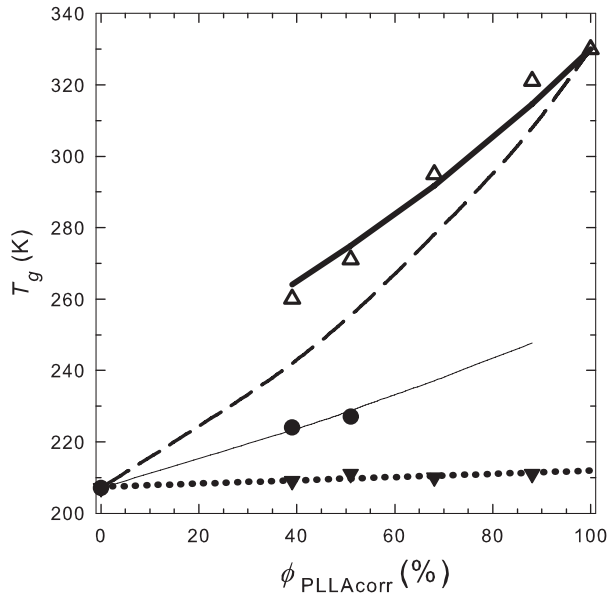

Fig. 6. T_g's compositional variation: of the bulk (Fox dependence) (– – –); of the experimental effective T_g's: $T_{g\ \mathrm{PLLA}}^{\mathrm{eff}}$ (△); $T_{g\ \mathrm{PCL}}^{\mathrm{eff}}$((▼) and (●)). Best fits: for $\phi_{\mathrm{s\ PLLA}} = 31\%$ (thick solid line), for $\phi_{\mathrm{s\ PCL}} = 100\%$ (• • • • •), for $\phi_{\mathrm{s\ PCL}} = 50\%$ (thin solid line).

a cooperative motion which is not perturbed by the presence of the PLLA component. The absence of miscibility in the amorphous regions of the copolymer should be accompanied by a segregation of the PLLA phase, leading to the presence of an α mode at the same temperatures than the α relaxation for neat PLLA. This is obviously not the case since the α_{PLLA} peak shifts to lower temperature continuously as the amount of PCL increases. The coexistence in the copolymers PLLA-*b*-PCL of at least two segmental modes, a composition-independent one and a composition-dependent one, is a new feature that was not found in miscible blends studied previously, where two T_g's were found both shifting in the temperature interval as the concentration of each blend component changed [24,25].

The existence of two cooperative mobilities is not by itself an indication of immiscibility of the amorphous phases. The self-concentration model proposed by Lodge and McLeish (LM) [13] for miscible blends predicts the existence of an effective T_g^{eff} for each blend component which can be quite different from the glass transition temperature corresponding to that of the bulk composition. They are attributed to a dynamic heterogeneity due to the average local composition perceived by each component in view of the chain connectivity. This model has been successfully applied to interpret TSDC results on polycarbonate, PC, and poly(ε-caprolactone), PC/PCL, blends [24] where two effective T_g^{eff}'s were detected, both of them composition dependent. Also in the case of the blends poly(styrene-co-maleic anhydride) containing 14% MA with PCL, PSMA14/PCL, two cooperative mobilities were detected in the TSDC spectra, both at intermediate temperatures between the homopolymers' T_g's [25]. The variation with composition of the two effective T_g^{eff}'s in both blends systems were quantitatively accounted for by using the Kuhn's length, ℓ_K, as the relevant length scale for the cooperative mobility and evaluating the self-concentration, ϕ_{s}, as

$$\phi_{\mathrm{s}} = \frac{C_\infty M_0}{k\rho N_0 \ell_K^3}\,, \tag{1}$$

where C_∞ is the characteristic ratio, M_0 is the repeat unit molar mass, k is the number of main chain bonds per repeat unit, ρ is the polymer density and N_0 Avogadro's number. A quantitative comparison between the experimental T_g's and the effective ones predicted by the LM model [13] is based on the calculation of the effective concentration for each component i:

$$\phi_i^{\mathrm{eff}} = \phi_{\mathrm{s}i} + (1-\phi_{\mathrm{s}i})\phi_i\,, \tag{2}$$

where ϕ_i is the crystallinity-corrected composition of the amorphous phase for each component in the blend. The model assumes that the composition variation of the two effective T_g^{eff} when using the effective concentrations follows for each composition the Fox equation. Then, $T_{g\ \mathrm{PCL}}^{\mathrm{eff}}$ and $T_{g\ \mathrm{PLLA}}^{\mathrm{eff}}$ can be calculated by

$$T_{g\ \mathrm{PCL}}^{\mathrm{eff}} = \left(\frac{\phi_{\mathrm{PCL}}^{\mathrm{eff}}}{T_{g\ \mathrm{PCL}}} + \frac{1-\phi_{\mathrm{PCL}}^{\mathrm{eff}}}{T_{g\ \mathrm{PLLA}}}\right)^{-1}. \tag{3}$$

In Figure 6 we have plotted the maximum of the TSDC α peaks, together with the bulk T_g compositional

variation calculated with Fox equation (dashed line) for a miscible blend. There is no possibility of comparing the calculated T_g Fox values to the DSC determined ones as the thermal history was different as will be explained below, and also because a measurable enthalpic step was not detected for all compositions in the DSC scans. It is to be noted that in Figure 6 the T_g's have been plotted as a function of the PLLA compositions in the amorphous phase, ϕ_{PLLAcorr}, *i.e.*, values corrected by taking into account the crystallinity degrees determined by WAXS. The data corresponding to the PCL component is almost independent of composition (▼) and consequently is very far from the bulk properties of a miscible blend. An inspection of the high-temperature side of the α_{PCL} TSDC peaks for the richest PCL contents shows the presence of a second peak which could be interpreted as a possible second glass transition mode located between the α_{PCL} and the α_{PLLA} peaks; it can be clearly seen for the $L_{32}C_{68}$ sample at $T = 222 \pm 2\,\mathrm{K}$ in Figure 4. For the $L_{55}C_{45}$ copolymer the peak is very wide and by changing the polarization conditions a peak at $227 \pm 3\,\mathrm{K}$ was found ((●) in Figure 6). These two TSDC responses were analyzed with the SADSA procedure and VTF elementary contributions had to be used to decompose the global curve, thus confirming the segmental character of these peaks, the best value for T_{VTF} being 150 K. Two Gaussian distributions could be identified in the analysis corresponding to $L_{32}C_{68}$ and $L_{55}C_{45}$ copolymers. The distribution at lower temperature had a mean VTF energy of 0.154 eV which is in excellent agreement with previous determinations on neat PCL [26]. For the two lower PCL contents, only very small irregularities were found.

The interesting question is: can this abundance of segmental mobilities in nearly disordered diblock copolymers, with distant glass transition temperatures and their variation with temperature, be explained by the LM Model? The TSDC technique is appropriate to test the model as we have already successfully showed in PC/PCL and PSMA/PCL blends [24,25]. With this technique the dielectric manifestation of the effective glass transition temperatures are intense peaks whose maxima can be precisely read. When using other techniques such as NMR, the changes in the T_g^{eff} have been sometimes estimated from the variation of the T_{VTF}, assuming that the other VTF parameters are not affected by blending, *i.e.* that the dynamics of blend components may be deduced from the neat homopolymers dynamics [27]. The calculation of the self-concentration for PLLA presents some problems due to the wide range of values for C_∞ found in the literature. From the lowest value given for the characteristic ratio in the pioneer works on the configuration statistics of PLLA chains [28,29], estimated both experimentally and theoretically, to the more recent work on PLLA [30,31] the reported C_∞ values ratio is 1.00 : 1.29 : 2.68. The two extreme sets of values lead to a range in the self-concentration values calculated from equation (1) from 47% to 8%. More recently, a RIS Metropolis Monte Carlo method has also been used to study PLLA where the polymer consistent force field was modified by reoptimizing some of its torsion parameters [32]. The value for $C_\infty = 5.67$ results from the calculation with the longest chain length (DP = 100) and if the modified field is chosen; the value for the PLLA self-concentration is then $\phi_{\mathrm{sPLLA}} = 35\%$. Due to this uncertainty, we decided to adjust our experimental results for $T_{g\mathrm{PLLA}}^{\mathrm{eff}}$ to equation (1) using ϕ_{sPLLA} as the single fitting parameter. This procedure has been previously used in dilute polymer blends by Lutz *et al.* [26] In Figure 6 the thick line represents the best fit to the data which is quite satisfactory, and the single parameter extracted from the fit is $\phi_{\mathrm{sPLLA}} = 31\%$.

For PCL, Figure 6 clearly shows the temperature invariance with composition of the lowest T_g component. In the original article on the self-concentration model [13] some qualitative conclusions were drawn about the relaxation time distributions. One of them is applicable here: PCL which is the faster and more flexible component might present a bimodal distribution, if the segmental mode is operating on a length scale that is smaller than the Kuhn's segment length. The excess volume may be occupied either by a single extra PCL chain, in which case the environment is pure PCL, or if it is taken by a PLLA chain, the local composition would then be 50 : 50. This predicted bimodal distribution could be the cause of the two α modes observed for the PCL component in PLLA-*b*-PCL. The two lines drawn at the bottom of Figure 6 represent the T_g^{eff} composition variation for PCL calculated for $\phi_s = 100\%$ (dotted line) and 50% (thin continuous line). The constant T_g^{eff} for PCL and the second segmental mode observed for the copolymers with the richest PCL concentrations is thus explained in the frame of the model which takes into account the chain connectivity.

A bimodal distribution has also been observed by dielectric spectroscopy and depolarized light scattering [33] in the diblock copolymer polystyrene and poly(methylphenyl siloxane), PS-*b*-PMPS. Kumar *et al.* [34] have proposed a model which explained the existence of heterogeneous environments for systems that are macroscopically homogeneous. It is based on the existence of local cooperative volumes of various sizes corresponding to local compositions and it also predicts that the faster component will have a bimodal distribution of relaxation times while the slower one will only exhibit a unimodal one. These cooperative volumes will diverge with $(T - T_0)^{-2}$, T_0 being the Vogel temperature.

3.3 DSC and PLOM evidences of miscibility

Additional evidence of miscibility by DSC and PLOM has been gathered. However, the comparison between the results obtained in this section and the TSDC results cannot be made quantitatively since the samples do not have identical thermal history and in the case of DSC, the polyesters tend to reorganize during the scan. For TSDC, samples have to be heated to a specific polarization temperature and then cooled down. In the case of the films employed for DSC measurements, the samples were simply cooled to −20 °C and then heated at 10 °C/min.

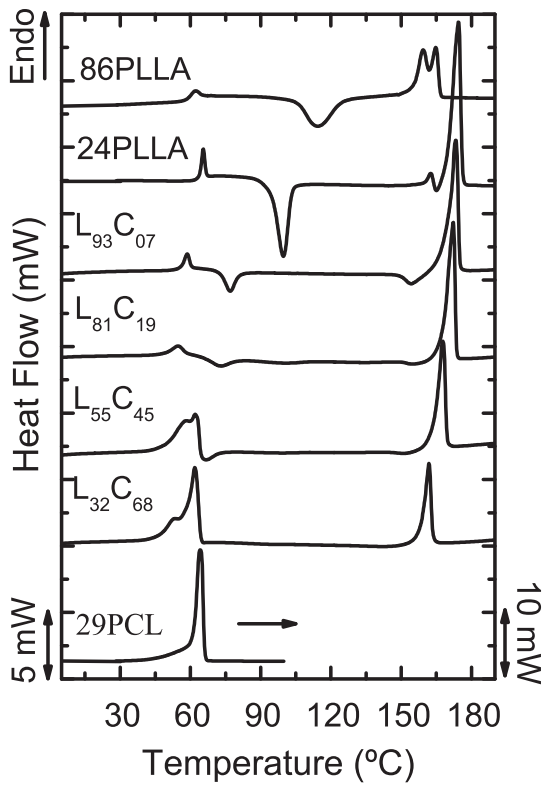

Fig. 7. DSC first heating scans from −20 °C at 10°C/min of compression-moulded films of PLLA-*b*-PCL diblock copolymers and corresponding homopolymers.

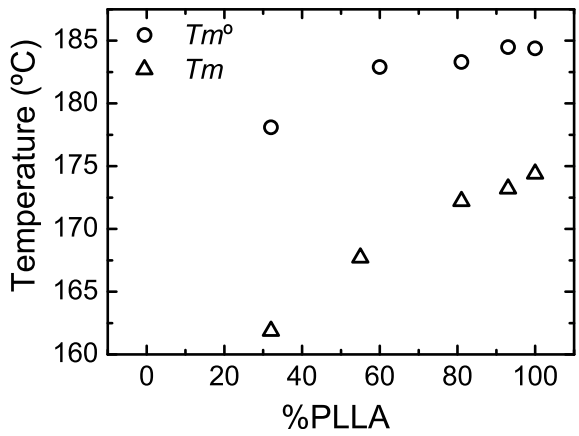

Fig. 8. Apparent melting temperatures obtained from Figure 7 and equilibrium melting temperatures (T_m^0) for PLLA-*b*-PCL diblock copolymers as a function of the bulk composition.

Figure 7 shows DSC first heating scans of the compression-moulded diblock copolymers and homopolymers films. It is interesting to note the differences between 24PLLA and 86PLLA. The fact that 86PLLA has a lower T_g and T_m values than 24PLLA indicates that the stereoregularity in 86PLLA is not as high as in 24PLLA as far as the content of the L stereoisomer is concerned. This can also explain why 86PLLA has a much lower crystallization rate than 24PLLA. The double melting peaks are a common feature of linear aliphatic polyesters that can reorganize during the scan, as well as the presence of cold crystallization exotherms.

The first endothermic small peak exhibited by 86PLLA and 24PLLA at a temperature close to 60 °C is due to an enthalpic relaxation process associated with the glass transition. In PLLA-rich copolymers ($L_{93}C_{07}$ and $L_{81}C_{19}$) a similar endothermic signal can also be seen although it is smaller and shifted to lower temperatures. The PCL block does not crystallize in these two samples as demonstrated by WAXS (Figs. 1 and 2). The depression of the T_g value as the PCL content in the copolymers increases observed in Figure 7, is consistent qualitatively with the TSDC results and with the miscibility of the amorphous phases. For samples with PLLA contents of 55% and 32% the T_g was not observed by DSC.

In the case of $L_{55}C_{45}$ and $L_{32}C_{68}$ the melting of the PCL block can be clearly seen as an endothermic double peak. The higher-temperature peak indicates the melting of the crystals formed during cooling from the melt (after compression moulding) while the lower temperature signal is due to room temperature annealing of the thinner lamellar population in the sample.

After the glass transition temperature of the PLLA block or the melting endotherm of the PCL block, usually two or more cold crystallization exotherms were observed. Some of the cold crystallization exotherms are not apparent in Figure 7 in view of the scale employed. The cold crystallization exotherms are due to the crystallization of the PLLA block, and they are also present in the heating scans of the PLLA homopolymers.

The peak crystallization temperature for the first cold crystallization process decreases progressively as the content of PCL in the diblock copolymers increases, from a value of 99.7 °C for 24PLLA to a value of 65.9 °C for the PLLA block within $L_{32}C_{68}$. Such a decrease is related to the T_g depression caused by the miscibility of the amorphous phases. For miscible systems the amorphous component with a lower T_g (in this case PCL) can act as a diluent decreasing the crystallization and melting temperature of the component that crystallizes and melts at higher temperatures (*i.e*, the PLLA).

From Figure 7 the melting temperature of the PLLA block was obtained and is plotted in Figure 8 as a function of the bulk composition. A continuous decrease in T_m is observed indicating a clear dilution effect possibly caused by miscibility of the amorphous components. These data are compared in Figure 8 with equilibrium melting temperatures (T_m^0) of the PLLA block. These values were calculated using the Hoffman-Weeks extrapolation on experimental data compiled after isothermal crystallization. The Hoffman-Weeks approach may not strictly apply in the case of block copolymers, since in the equilibrium state a folded chain configuration in the lamellar crystals may prevail [35]. Nevertheless, the Hoffman-Weeks plots yielded very good straight lines with correlation coefficients larger than 0.98, and they were employed in a comparative way. A reduction in T_m^0 is also obtained; this

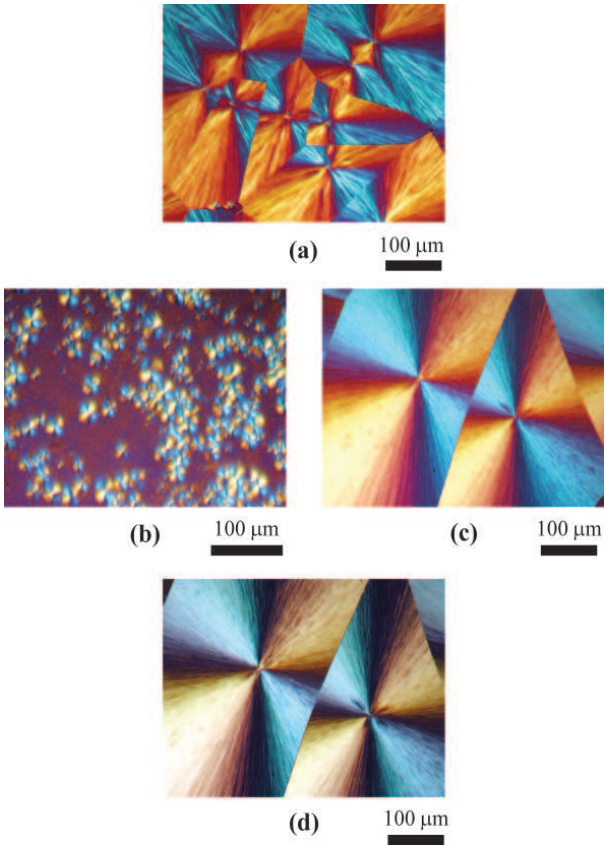

Fig. 9. Polarized-light micrographs of (a) 24PLLA homopolymer crystallized isothermally at 130 °C until saturation; (b) $L_{55}C_{45}$ film quenched from the melt; (c) $L_{55}C_{45}$ film crystallized isothermally at 130 °C until saturation; (d) same sample as in (c) after PCL crystallization at 40 °C.

is a strong indication of the dilution effect caused by PCL on PLLA in view of their miscibility.

Figure 9 shows a series of PLOM micrographs. In the case of the 86PLLA films obtained by compression moulding, the morphology was featureless since it was almost completely amorphous (result not shown). In the diblock copolymer cases, because the PLLA block has a much lower molecular weight, a spherulitic morphology was always observed. Since the films employed in the TSDC experiments were compression moulded and quickly quenched from the melt, only small spherulites were obtained and a representative micrograph of the superstructural morphology of the diblock copolymer films is shown in Figure 9(b) for the $L_{55}C_{45}$ diblock copolymer.

With the purpose of demonstrating the mixed spherulitic morphology obtained in the diblock copolymer films, isothermal crystallization was performed in order to obtain large spherulites and they are shown in Figure 9. At 130 °C, the spherulites of 24PLLA are shown after they have impinged in Figure 9(a) and they can be compared with those obtained by isothermal crystallization at the same temperature in $L_{55}C_{45}$. At 130 °C, the PCL block is molten, and therefore the spherulites observed in $L_{55}C_{45}$ are semicrystalline units, where PLLA block crystalline lamellae have grown radially and in the interlamellar regions a miscible phase of PCL block and PLLA block amorphous chains are located (the PCL block molten chains amount to 45% by weight of the material). Figure 9(d) shows the morphology of the same sample after it was quenched to 40 °C and left at that temperature during 30 min for the PCL block to crystallize until saturation. The crystallization of the PCL block does not change significantly the superstructural features imposed by the previous crystallization of the PLLA block, but the birefringence was decreased to more negative values (these spherulites are negative) indicating the presence of PCL block crystals. On a microscopic level the crystallization of the PCL block can lead to partial melting of PLLA block at the lamellar interface as documented by simultaneous SAXS/WAXS studies recently reported [9,10]. The formation of mixed spherulites is typical of diblock copolymers that are weakly segregated or melt mixed [12]. PLOM experiments have shown that the crystallization of the PLLA block within the diblock copolymers occurs at higher temperatures as the sample is cooled from the melt and it forms spherulites that template the morphology. The PCL block is left to crystallize at lower temperatures in the interlamelar regions within the spherulites already formed by the PLLA block. When the content of PLLA is large, the PCL block crystallization is topologically confined within these intra-spherulitic regions and its degree of crystallinity is substantially reduced [9,10].

4 Conclusions

The study of the dynamics of a diblock copolymer, PLLA-*b*-PCL, with two crystalline blocks by the TSDC technique has shown a complex behavior with several segmental modes in the wide interval between the two T_g's of the homopolymers, $\Delta T_g = 123$ K. PLLA has an effective glass transition temperature which decreases with the PCL concentration as expected by the LM model for miscible blends. This important decrease is accompanied by two PCL effective glass transition temperatures: one that is invariant with composition and a second one that is visible for the copolymers with the richest PCL concentrations. The latter one varies with concentration in agreement with a 50% value for the PCL self-concentration as predicted by the LM model for the faster component. Our experimental results agree well with this model, the self-concentrations found being $\phi_{\mathrm{sPLLA}} = 31\%$, $\phi_{\mathrm{sPCL}} = 100\%$ and 50%. The miscibility in the amorphous phase of the two components is thus confirmed and the presence of multiple glass transitions explained with the LM model. Also the low temperature or secondary modes show important changes as compared to the homopolymers which indicate that the presence of PCL affects seriously the number of orientable dipoles in the material. The shortest-range motions are enhanced by the addition of small quantities of PCL, while the pre-cooperative motions of PLLA which are at the origin of the β relaxation are somewhat constrained by the presence of PCL. The more important modification of the secondary relaxation profile of the PLLA in the presence

of PCL than in the opposite situation confirms the presence of nanoscale domains where the composition is near 100% PCL. The miscibility in the amorphous phase on a macroscopic and microscopic scale has been confirmed by the compositional dependence of the glass transition and melting temperature of the PLLA blocks determined by DSC, and by the PLOM studies that have shown a mixed spherulitic morphology typical of melt mixed diblock copolymers (or in the weak segregation regime).

This work was supported by the Fondo Nacional de Investigaciones Científicas y Tecnológicas (Proyectos FONACIT F-2005-000284, G-2005-000776) and the Universidad Simón Bolívar (DID-G15 and DID-G02). This work was partly supported by the Belgian Federal Government Office of Science Policy (SSTC-PAI 5/3).

References

1. J. Albuerne, L. Márquez, A.J. Müller, J.M. Raquez, Ph. Degée, Ph. Dubois, V. Castelletto, I. Hamley, Macromolecules **36**, 1633 (2003).
2. A.J. Müller, J. Albuerne, L. Márquez, J.M. Raquez, Ph. Degée, Ph. Dubois, J. Hobbs, I.W. Hamley, Faraday Discuss. **128**, 231 (2005).
3. J. Albuerne, L. Márquez, A.J. Müller, J.M. Raquez, Ph. Degée, Ph. Dubois, Macromol. Chem. Phys. **206**, 903 (2005).
4. S. Nojima, Y. Akutsu, M. Akaba, S. Tanimoto, Polymer **46**, 4060 (2005).
5. J. Sun, Z. Hong, L. Yang, Z. Tang, X. Chen, X. Jing, Macromolecules **45**, 5969 (2004).
6. J.K. Kim, D.J. Park, M.S. Lee, K.J. Ihn, Polymer **42**, 7429 (2001).
7. C. He, J. Sun, T. Zhao, Z. Hong, X. Zhuang, X. Chen, X. Jing, Biomacromol. **7**, 252 (2006).
8. T. Shiomi, K. Imai, K. Takenaka, H. Takeshita, H. Hayashi, Y. Tezuka, Polymer **42**, 3233 (2001).
9. I.W. Hamley, P. Parras, V. Castelletto, R.V. Castillo, A.J. Müller, E. Mollet, Ph. Dubois, C.M. Martin, Macromol. Chem. Phys. **207**, 941 (2006).
10. I.W. Hamley, V. Castelletto, R.V. Castillo, A.J. Müller, C.M. Martin, E. Pollet, Ph. Dubois, Macromolecules **38**, 463 (2005).
11. A.J. Müller, V. Balsamo, M.L. Arnal, Adv. Polym. Sci. **190**, 1 (2005).
12. A.J. Müller, V. Balsamo, M.L. Arnal, Lect. Notes Phys. **714**, 229 (2007).
13. T.P. Lodge, T.C.B. McLeish, Macromolecules **33**, 5278 (2000).
14. Y. He, T.R. Lutz, M.D. Ediger, Macromolecules **36**, 8040 (2003).
15. Y. He, T.R. Lutz, M.D. Ediger, T.P. Lodge, Macromolecules **36**, 9170 (2003).
16. Ph. Dubois, C. Jacobs, R. Jerome, Ph. Teyssie, Macromolecules **24**, 3027 (1991).
17. E. Laredo, A. Bello, M.C. Hernandez, M. Grimau, J. Appl. Phys. **90**, 721 (2001).
18. H. Bittiger, R.H. Marchessault, W.D. Niegisch, Acta Crystallogr., Sect. B **26**, 1923 (1970).
19. S. Sasaki, T. Asakura, Macromolecules **36**, 8385 (2003).
20. E. Laredo, N. Suarez, A. Bello, B. Rojas, M.A. Gomez, J.M.G. Fatou, Polymer **40**, 6405 (1999).
21. K.L. Ngai, M.J. Paluch, Chem. Phys. **120**, 857 (2004).
22. G.P. Johari, M.J. Goldstein, Chem. Phys. **53**, 2372 (1970).
23. M. Grimau, E. Laredo, M.C. Pérez Y., A. Bello, J. Chem. Phys. **114**, 6417 (2001).
24. D. Herrera, J.C. Zamora, A. Bello, M. Grimau, E. Laredo, A.J. Müller, T.P. Lodge, Macromolecules **38**, 5109 (2005).
25. V. Balsamo, D. Newman, L. Gouveia, L. Herrera, M. Grimau, E. Laredo, Polymer **47**, 5810 (2006).
26. E. Laredo, A. Bello, M. Grimau, Polym. Bull. **42**, 117 (1999).
27. T.R. Lutz, He Yiyong, M.D. Ediger, M. Pitsikalis, N. Hadjichristidis, Macromolecules **37**, 6440 (2004).
28. A.E. Tonelli, J. Flory, Macromolecules **2**, 225 (1969).
29. D.A. Brant, A.E. Tonelli, P.J. Flory, Macromolecules **2**, 228 (1969).
30. C.A.P. Joziasse, H. Veenstra, D.W. Grijpma, A.J. Pennings, Macromol. Chem. Phys. **197**, 2219 (1996).
31. D.W. Grijpma, J.P. Penning, A.J. Pennings, Colloid Polym. Sci. **272**, 1068 (1994).
32. J. Blomqvist, Polymer **42**, 3515 (2001).
33. S.H. Anastasiadis, G. Fytas, S. Vogt, B. Gerharz, E.W. Fischer, Europhys. Lett. **22**, 619 (1993); G. Meier, D. Vlassopoulos, G. Fytas, Europhys. Lett. **30**, 325 (1995).
34. S.K. Kumar, R.H. Colby, S.H. Anastasiadis, G. Fytas, J. Chem. Phys. **105**, 3777 (1996).
35. E.A. DiMarzio, C.M. Guttman, J.D. Hoffman, Macromolecules **13**, 1194 (1980).